

LUMINESCENCE DATING OF ENIGMATIC ROCK STRUCTURES IN NEW ENGLAND, USA

Dr. James K. Feathers, University of Washington

Department of Anthropology

Enigmatic rock structures, in the form of walls, cairns, tunnels and chambers, made by piling up locally available rocks, are common archaeological features in northeastern United States. One list mentions 5550 such sites (Hoffman, 2019). Professional archaeologists have traditionally attributed these structures to European colonial activity (Ives, 2013,2015), but others, principally interested amateurs and some native Americans, maintain they have prehistoric origins (e.g., Moore and Weiss, 2016). Chronological evidence is scarce: associated artifacts are rare and a handful of radiocarbon dates have uncertain associations. Luminescence dating, applied to sediments associated with a stone structures in Massachusetts and Rhode obtained dates in the prehistoric range of AD 1450-1650 (Mahan et al. 2015, Mahan, 2019). Here we report results of a systematic luminescence study dating sediments and stones in New England.

1. Samples

More than 40 samples have been collected from more than 20 rock structure sites from seven states. This report is limited to 12 sediment samples and five rock samples from nine of these sites in Rhode Island, Connecticut, New Hampshire, and New York (Table 1). Maps and photos of the sampling locations are given in the supplemental data.

UW lab #	Site	State	Structure type	Sample type
UW4076	Madison Lithic	CT	wall	Sediment-pipe
UW4077	Madison Lithic	CT	Small platform	Sediment-pipe
UW4080	Gungywamp	CT	wall	rock
UW4081	Gungywamp	CT	chamber	Sediment-pipe
UW4083	Hunt's Brook Souterrain	CT	chamber	Sediment-pipe
UW4084	Hunt's Brook Souterrain	CT	tunnel	rock
UW4087-8*	Manitou Hassannash	CT	wall	Sediment-pipe/trowel
UW4089	Manitou Hassannash	CT	cairn	Sediment-trowel
UW4091	ED Wood Estate	RI	cairn	rock
UW4092	Lewis Hollow	NY	cairn	Sediment-trowel
UW4095	Slatersville Rocky Hill Rd	RI	wall	Sediment-trowel
UW4098	America's Stonehenge	NH	chamber	Sediment-pipe
UW4099	America's Stonehenge	NH	chamber	rock
UW4100	America's Stonehenge	NH	tunnel	rock
UW4101	America's Stonehenge	NH	wall	Sediment-trowel
UW4102	Crown Farm	RI	wall	Sediment-trowel

Sediment samples, in all but one case, were collected directly underneath a rock forming part of the structure. At first, these were collected by driving a 2.5 cm diameter steel pipe horizontally under the rock to control the depth of the sample, but this proved difficult because buried rocks were

encountered. Subsequently, samples were collected by trowel and shielded from light by an opaque tarp. For one sample (UW4087-UW4088) both methods were used adjacent to each other. The exception to collecting under a rock is UW4098, which was collected from sediment on top of the main chamber at America's Stonehenge. This will provide only a minimum age for the chamber.

The sediments directly beneath the rocks formed the ground surface prior to building the structure. At that time, bioturbation (mainly from tree fall, I suspect, given the forested environment) continually brought grains to the surface where they were exposed to sunlight (Feathers et al. 2015). With rock placement, grains were no longer brought to the surface, staying buried, thus providing a way to date this placement. Because only some grains were fully exposed before rock placement, only the youngest grains will provide an accurate date.

Rock samples were collected directly from an inside portion of the structure under an opaque tarp. Presumably the rocks were exposed to light during construction so dating a surface not exposed now within the structure should date the construction.

2. Methods

The luminescence signal of minerals such as quartz and feldspar is a function of natural radioactivity. The intensity of the signal is proportional to age. The amount of radiation necessary to produce the natural luminescence signal (called the palaeodose) is estimated using laboratory irradiation as an equivalent dose (D_e). Dividing that by the dose rate gives the age since the last time the signal was set to zero, usually by heat or exposure to sunlight. The dose rate (Gy per unit time) is the rate at which irradiation is absorbed by the sample in its natural setting. It depends on the radioactivity of the sample and its immediate surroundings.

Dose rate – Natural radiation is composed of alpha, beta, gamma and to some extent cosmic radiation. For coarse-grained material in high radiation environments such as the case here, the bulk of the dose rate comes from beta and gamma radiation. Betas are relatively short-ranged and stem mainly from the sample itself, but gammas have a range of about 30 cm in sediments and rocks. In complicated geometries such as these rock structures the gammas can arise from sediments and rocks in the near vicinity. These may vary considerably in their radioactivity. For example, in one cairn that was measured, rocks varied in their potassium (K) content (^{40}K is a principle source of natural radioactivity) from 1.5 to 7%.

Two approaches to estimating the gamma dose rate were applied. One was to collect a sample of sediments and rocks within about 20 cm of the sample, measure their radioactivity in the laboratory, and use the geometry to reconstruct the dose rate (following Aitken 1985, appendix H, using a density of 1.5 for the sediment and 2.6 for the rocks). The other was to place a $\text{CaSO}_4:\text{Dy}$ dosimeter at the approximate location of the sample and leave it there for one year. A drawback of the laboratory method, besides the complicated geometry, is that one cannot see and thus sample what is behind the sample. A drawback of the dosimetry method is that it is difficult to place the dosimeter exactly where the sample was. It was placed in the hole from which the sample was drawn but only at one point while the sample was taken over an area. The radioactivity can vary in this environment over short distances.

For example, the calculated dose rates for UW4087 and UW4088, only 10 cm apart, varied from 3.6 to 4.3 Gy/ka. Most confidence was placed in those samples where the two approaches produced statistically identical dose rates. For the dated rocks, some of the beta dose also comes from outside the sample. There was another rock directly underneath the surface being dated. Half the beta dose rate to the surface will come from this other rock. The average of both rocks can be used for the age at the surface, but with depth, the beta dose increasingly comes from the dated rock. After a couple of millimeters all of it does. For UW4091 (the only sample where this matters) such adjustments made a difference of less than 1%. For the dated rocks dosimeters were only placed for UW4084 and UW4099. For these it was not possible to collect adjacent rocks for laboratory measurements without doing damage to the structure. No dosimeter was placed for the other rocks, because there was no practical way to retrieve them (e.g., deep in a cairn). Grain size of the rocks was not measured, but the rocks were coarse grained and it was assumed grain size averaged 150-250 μ m for purposes of calculating alpha and beta attenuations.

Because single grains were dated for the sediments, a further consideration for the beta dose rate is heterogeneity in the distribution of beta emitters. Some grains will receive a higher dose rate than others because they are closer to an emitter. For K-feldspars, much of this variation probably arises from variation in the percentage of internal K (^{40}K is a major beta emitter), which can vary from a few to 14%. Internal K was not measured on these samples, but following Smedley et al. (2012) we assumed an average internal K content of 10%, although increased the one-sigma error to 3% to cover more possibilities. For quartz, a likely source of beta heterogeneity is the K-feldspar grains, which can have an uneven distribution if not abundant. The distribution of K “hotspots” was modelled after Mayya et al. (2006) and Chauhan et al. (2021), taking into account the beta dose rate and the percentage of betas stemming from K, to see how much over-dispersion in D_e could be potentially explained by beta heterogeneity. This could have some bearing on the minimum age model used to determine D_e .

Moisture contents were estimated from measured current values, which varied from 1 to 9%, although at least 3% was assumed. The samples were relatively dry, being situated under rocks or in structures. Laboratory measurements of dose rate used alpha counting, beta counting and flame photometry.

Equivalent dose – For the sediments, luminescence was measured on 180-212 μ m single grains of K-feldspar and quartz. These were prepared following standard procedures, including wet and dry sieving, treatment with HCl and H_2O_2 , and density separation using heavy liquids of 2.58 and 2.66 specific gravity for K-feldspars and quartz respectively. Quartz was additionally etched for 40 min in 48% HF. Given the low sensitivity of quartz noted in the literature for Quebec (using UV filters), we originally thought that only K-feldspars would be used, but quartz for all samples had a measurable signal in the UV. Measurements were made on Risø TL/OSL-DA-20 reader, using infrared stimulated luminescence (IRSL) for feldspars and optically stimulated luminescence (OSL) for quartz. Stimulation of the K-feldspars was by a 150 mW 830nm IR laser, set at 30% power and passed through a RG780 filter. Stimulation of quartz was by a 540 nm green laser (45W/cm²) at 90% power. Emission for K-feldspars was through a blue filter pack (350-450 nm) and for quartz through a UV340 (ultraviolet) filter. The

signal was collected for 0.8 s, with the first 0.06 s used for analysis and the last 0.15 s for background. D_e was determined using the single-aliquot regenerative (SAR) protocol (Murray and Wintle 2000, Auclair et al. 2003). Regeneration doses of from 1 to 20 Gy and test dose of 3 Gy were employed. Laboratory doses were provided by a ^{90}Sr beta source, calibrated at each single-grain position using quartz gamma-irradiated at Pacific Northwest National Laboratory, Hanford, WA. A preheat of 250°C for 1 m was employed for K-feldspars after both regeneration and test doses. For quartz a preheat of 240°C for 10 seconds was employed after regeneration doses and a 200°C cut heat after test doses. The IRSL protocol included after every cycle a high temperature (325°C) stimulation using IR diodes for 40s to reduce signal carry over. Zero dose and repeat regeneration doses were used to detect violation of the SAR assumptions, and grains that did not meet these criteria were removed from analysis along with any grains that lacked a measurable signal, had a natural signal that did not intersect the regeneration growth curve, and for quartz, any grains deemed to be feldspars by a response to an IR stimulation after two regeneration doses. A dose recovery test to see if known doses can be obtained with the protocol was performed for both minerals.

K-feldspar suffers from a loss of signal at ambient temperature called anomalous fading. For older samples, a high temperature IR stimulation, in a method called post-IR-IR (pIRIR), is commonly used to circumvent fading, but the pIRIR signal is known to be difficult to bleach (Buylaert et al. 2012). Because these samples are young and we wanted to be sure some grains were well bleached, we did not use it. Instead, we corrected for fading using the Huntley-Lamothe (2001) method, which seems to work well for young samples. Fading was corrected on every grain following procedures by Auclair et al. (2003), using regeneration doses of about 30 Gy, test doses of about 10 Gy, and storage times up to 3 days or longer.

Because only some of the grains in the samples are apt to be well-bleached, we utilized the minimum age model (Galbraith and Roberts 2012) to determine the D_e of the youngest grains. The central age model for central tendency and the finite mixture model for the structure of the distribution (Galbraith and Roberts 2012) were also employed for comparison. Radial graphs of the distributions were constructed for every sample.

For the rocks, at least three 1.5 cm cores were drilled into unexposed surfaces using a diamond tipped drill bit mounted on a drill press under red light conditions. The cores were then sliced into ~1 mm slices using a Pace Technology precision saw with a 400 μm diamond studded blade. Because some of the rocks were rather friable, the cores were first impregnated in epoxy before cutting. The rocks were coarse-grained granitic gneiss. Portions of each slice were measured for luminescence on a Risø TL/OSL-DA-15 reader. D_e was determined by the double SAR method (Banerjee et al. 2001), where an infrared stimulation proceeded a blue stimulation, both using diodes and for 100 s at each step. Emission was through a UV340 filter, and the preheat and test dose were the same as those used for quartz described earlier. A fading test was performed on all slices.

3. Results

Dose rate -- Table S1 gives the relevant concentrations provided by alpha counting and flame photometry. Table S2 compares the beta dose rate determined in two ways, compares the gamma (plus cosmic) dose rates between laboratory and field measurement (dosimeters), and lists the total dose rate for both quartz and k-feldspar. The beta dose rate was calculated from flame photometry and alpha counting assuming secular equilibrium and also measured directly by beta counting. These differed significantly for only a handful of samples (marked in italics in S2), most seriously for UW4092. The problem in all cases seemed to be an error in K measurement. The dose rate was adjusted for these samples to agree with the beta counting.

Figure 1 compares the gamma and cosmic dose rates between laboratory measurements and the field measurements from the dosimeter. The data are from Table S2. Of the 12 comparison, 5 are within error terms, 3 are relatively close and four are quite different. (The data for UW4102 are not plotted because the dosimeter reading for this sample was abnormally high, twice that of the next highest reading.) The dosimeter readings are also systematically higher (in all cases but one) than the laboratory measurements. We also noticed this on two samples, measured at the same time, from southwestern Washington state, where the deposits are fairly homogeneous. We do not have a reason for this bias, but it is possible the dosimeters are over-estimating the dose rate, although as will be seen only four samples present a significant difference between the two measures, and of those four three using the dosimetry measurements produced ages consistent with other samples. The effect of the dosimeter measurements on the final dose rates was judged by a comparison of dose rates for K-feldspar (Table S2). The final dose rates comparing lab and dosimeter measures for the gamma/cosmic dose rate, on the 11 samples where such a comparison could be made, do not differ at one-sigma for five samples, at two-sigma for four samples, and are really only a problem for UW4076, UW4089 and UW4102, although for UW4092 the agreement at two-sigma is only because of high errors. The issue will be considered further when calculating ages.

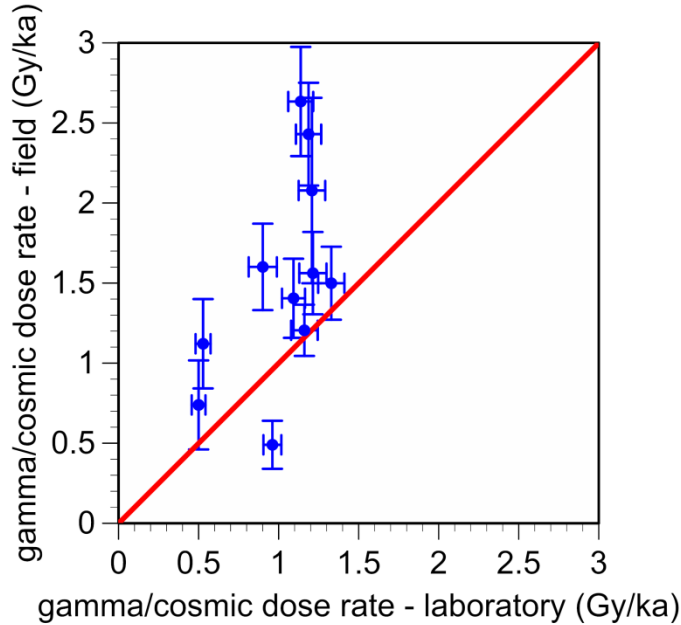


Figure 1. Comparison of gamma and cosmic dose rates between the laboratory measurements and the field measurements (dosimeter). The red line is 1:1 correspondence.

Equivalent dose and age – K-feldspars – Table 2 gives the number of accepted grains, the D_e values, over-dispersion and the average fading rate for each sample. The samples were relatively sensitive: 32% of all grains passed the rejection criteria and were accepted for analysis. Most of the rejections were due to poor signals. Some grains, about 2 percent of all grains, were rejected because D_e was not significantly different from zero. While these may have some bearing on the age of these young samples, most of them were poor precision grains that would not affect over-all statistics. The over-dispersion, which is a statistical measure of the spread in values, was very high, more than 100% for most samples. While some of this may reflect differential fading, the most likely explanation is a wide dispersion in ages, supporting the idea that only some of the grains were well bleached at the time of rock placement. Average fading rates vary widely among samples. This reflects the wide range of fading values commonly seen in single-grain data. High errors on fading rates are characteristic of single-grains, but other work by this lab (Feathers et al. 2019) has shown that fading rates on individual grains are broadly reproducible. Summary statistics such as those provided by the various age models are particularly reproducible.

Table 2. D_e and other data for K-feldspars

Sample	# accepted grains	D_e (Gy)	Over-dispersion (%)	Fading rate, g, (%/decade) Weighted average
UW4076	166	1.70±0.13	93.8	2.67±0.80
UW4077	103	3.40±0.43	117.5	1.87±0.71
UW4081	250	7.18±0.55	118.2	4.09±0.40

UW4083	182	10.5±0.90	111.3	5.59±0.58
UW4087	244	2.44±0.31	127.2	8.69±0.96
UW4088	116	3.33±0.43	126.2	6.47±0.73
UW4089	177	3.86±0.28	86.4	6.19±0.48
UW4092	155	2.86±0.32	133.2	8.61±0.66
UW4095	112	3.65±0.46	121.2	3.31±0.77
UW4098	234	4.92±0.38	110.5	2.92±2.78
UW4101	106	6.46±0.70	103.1	1.64±5.45
UW4102	128	3.55±0.37	111.4	6.31±0.80

Table 3 gives the ages -- corrected for fading using the Huntley-Lamothe (2001) method -- from the central age model and the minimum age model, plus the over-dispersion. The ages were calculated for most samples using the laboratory derived dose rates, but for samples where using the dose rate from the dosimetry data made a significant difference in age the ages from the latter are also given. The distributions are displayed as radial graphs in Figure S3.

The over-dispersion values for the ages are similar to those for equivalent dose. This suggests the over-dispersion is not the result of differential fading. It is more likely a function of differential age, justifying the use of the minimum age model to determine the age of rock placement. The minimum age model requires the input of an over-dispersion value considered typical of a single-aged sample. A dose recovery test was performed on grains from four samples. The same dose is given to all grains, so this represents a single-aged sample. When three high outliers and one low outlier were removed, the remaining 33 grains that were accepted gave a ratio of derived to administered dose of 1.06 ± 0.04 with an over-dispersion of 6%. This is satisfactory but the over-dispersion is under-estimated because of the removal of outliers. An over-dispersion value of 15% was used for the minimum age model. The minimum age model can be run with three or four unknowns. Both were attempted, but using four unknowns either produced the same value as using three unknowns or resulted in poor fits for most samples.

For three of the samples where ages derived using the dosimetry data are given, these ages are more in align with the ages from the other samples. This implies the dosimeters gave a more accurate gamma dose rate than the laboratory measurements did. For the fourth sample, UW4102, which had a very high dosimeter reading, the age using the dosimetry information gave an age of AD1880, probably young enough for the structure to have a written record of its construction, which it does not have. The dosimeter is probably inaccurate. Overall, the ages are remarkably consistent. The ages for the three samples using the dosimeter information and the ages of all others using only laboratory measurements (leaving out UW4088), yields a weighted average age of 0.43 ± 0.02 ka, or AD 1590 \pm 20, with no over-dispersion. That means all ages are statistically consistent with a single-age, which is 30 years before the first European settlers arrived. UW4088 has an anomalously young age. This sample was collected by trowel only 10 cm from UW4087 which was collected using a pipe. The ages from the central age model are similar, but UW4087 just did not have the large number of very young grains that UW4088 did. Possibly this means that modern grains found their way into this sample, although other samples collected with a trowel did not have this problem.

Table 3. Age data for K-feldspars

Sample	Age (ka) Central age model	Over-dispersion %	Age (ka) minimum age model	Calendar date (years AD)
UW4096	1.37±0.15	96.1	0.54±0.08	1480±80
With dosimeter	0.98±0.11	94.7	0.39±0.06	1630±60
UW4077	2.02±0.29	114.9	0.37±0.07	1650±70
UW4081	2.74±0.23	113.4	0.46±0.05	1560±50
UW4083	3.36±0.37	108.4	0.48±0.08	1540±80
UW4087	0.90±0.14	96.3	0.46±0.11	1560±110
UW4088	0.80±0.08	112.3	0.24±0.07	1780±70
UW4089	1.44±0.13	76.2	0.59±0.01	1430±70
With dosimeter	1.08±0.10	76.6	0.40±0.07	1620±70
UW4092	1.76±0.26	128.8	0.66±0.07	1360±70
With dosimeter	1.14±0.16	126	0.43±0.05	1590±50
UW4095	1.12±0.15	111.7	0.33±0.07	1690±70
UW4098	2.17±0.20	113.6	0.41±0.05	1610±50
UW4101	2.28±0.27	99.8	0.55±0.10	1470±100
UW4102	1.54±0.22	106.5	0.40±0.10	1620±100
With dosimeter	0.60±0.09	112.8	0.14±0.03	1880±0.03

The shape of the radial graphs can inform on the likelihood that the minimum age model isolates well bleached grains. There are two general patterns in the graphs. One, represented by UW4092 in Figure 2, is a somewhat bimodal distribution, showing a large number of grains consistent with the minimum age model and a smattering of older grains. Seven of the samples have this kind of distribution. The other pattern, represented by UW4081 in Figure 2, does not show much of a clump at the young end but rather a more or less even distribution throughout the age range. Five show this pattern. The clumping at the young end of the bimodal distributions suggests that these grains represent the youngest possible grains. There are no points below the bottom line in the graph, which seems to act as a barrier. I argue these grains are well bleached. That is less clear for UW4081. There could be younger grains. However, because there is no difference in minimum ages between the two patterns, it is likely the youngest grains in all samples are well bleached. The older grains in the distributions seem to give Late Pleistocene ages, which is probably the age of the landform the structures sit on.

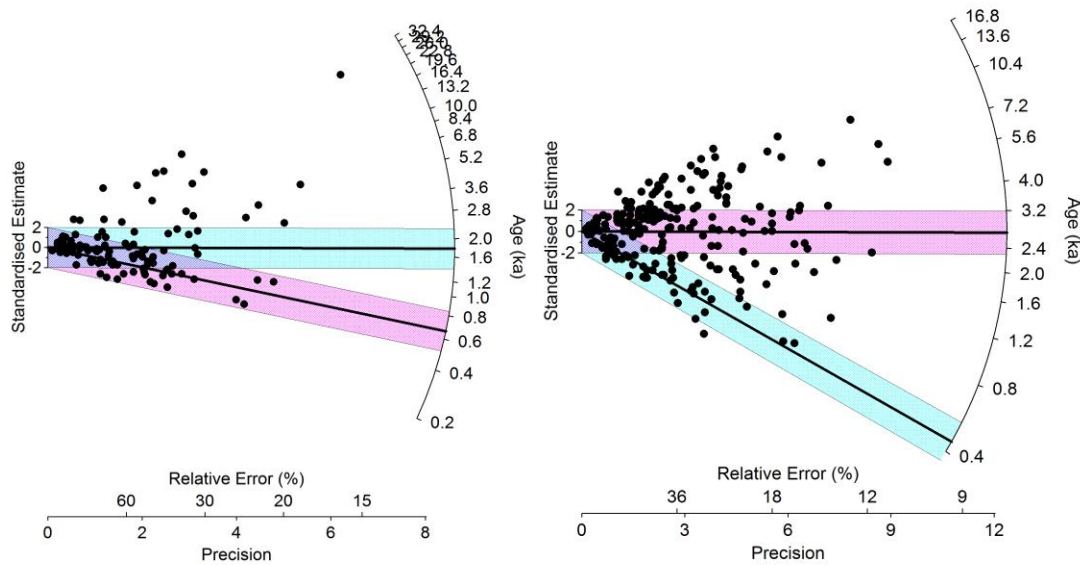


Figure 2. Radial graphs for the age distribution of K-feldspar grains in UW4092 (left) and UW4081 (right). UW4092 shows a bimodal distribution, while UW4081 shows a more continuous distribution.

Equivalent dose and age – quartz. Table 4 gives the number of grains accepted, the D_e from the central age model, the over-dispersion, and the D_e from the minimum age model. Quartz was much less sensitive than the K-feldspar, as is typical. Only 9 % of grains passed the acceptance criteria (compared to 32% for K-feldspar) and it took a lot of machine time to get a statistically large enough sample. A vast majority of the rejects were for poor signal.

Table 4. D_e and other data for quartz

Sample	# accepted grains	D_e (Gy) Central age model	Over-dispersion (%)	D_e (Gy) Minimum age model
UW4076	66	2.40±0.24	68.2	0.98±0.16
UW4077	89	1.53±0.20	116.1	0.44±0.07
UW4081	78	5.25±0.76	120.1	0.8±0.08
UW4083	49	4.40±0.81	116.4	1.20±0.34*
UW4087	108	1.46±0.18	114.9	0.64±0.04
UW4088	43	0.88±0.13	86.0	0.61±0.05
UW4089	68	4.07±0.52	96.7	0.75±0.08
UW4092	100	1.54±0.18	103.7	0.53±0.09
UW4095	91	2.08±0.26	109.6	0.90±0.05
UW4098	72	2.35±0.35	113.9	0.79±0.15
UW4101	156	3.23±0.25	89.6	0.89±0.09
UW4102	63	2.09±0.32	117.2	0.47±0.10

* One outlying point removed

A dose recovery test was done on seven samples, and 88 grains passed the acceptance criteria. The ratio of derived to administered dose was 1.04 ± 0.3 , again satisfactory, with 9% over-dispersion. An over-dispersion value of 15 % was assumed typical of a single-aged sample for the minimum age model, although this value will be re-evaluated later. Radial graphs are shown in Figure S4. Most samples have the bimodal pattern, so the young grains are probably well bleached. Ages are given in Table 5. The ages are computed using the laboratory dose rate data, except for the minimum age for UW4076, UW4089 and UW4092 where the dosimetry data were used, as justified in the discussion on K-feldspars.

Table 5. Quartz ages.

Sample	Age (ka) Central age model	Age (ka) Minimum age model	Calendar age (years AD)
UW4076	2.69±0.33	0.66±0.16	1360±160
UW4077	1.22±0.18	0.35±0.06	1670±60
UW4081	1.88±0.29	0.29±0.03	1730±30
UW4083	1.31±0.25	0.36±0.10	1660±100
UW4087	0.48±0.06	0.21±0.02	1810±20
UW4088	0.24±0.04	0.17±0.02	1850±20
UW4089	1.33±0.18	0.17±0.02	1850±20
UW4092	0.65±0.09	0.14±0.03	1880±30
UW4095	0.71±0.10	0.31±0.03	1720±30
UW4098	1.12±0.19	0.38±0.08	1640±80
UW4101	1.34±0.12	0.37±0.04	1650±40
UW4102	0.89±0.15	0.20±0.04	1820±40

The quartz ages from the minimum age model are systematically younger than the K-feldspar ages, except for UW4076 (Figure 3). Many are colonial in age, but others are post-colonial, dating to the 19th century, later than even those who support a colonial era origin for the structures would argue. Moreover, unlike the K-feldspar dates, the quartz dates are not statistically consistent with a single date. The reasons for the differences between the feldspar and quartz ages will be taken up later.

Equivalent dose and age – rocks. Of the five rocks measured, three of them, UW4080, UW4099 and UW4100, yielded very high D_e values at the surface of the rock. This indicates the rocks were not well-bleached at the time of their placement. Only data from the other two rocks, UW4084 and UW4091, are presented. The double SAR method provides a D_e value for both IRSL and OSL. The OSL signal was poor on both rocks. Only on one core from UW4091 did the signal pass the acceptance criteria. The focus here then is on the IRSL signal. Table S3 gives the IRSL D_e and \ln/T_n (signal ratio between the natural and first test dose) as a function of depth for two cores from each sample and the OSL D_e and \ln/T_n for one core from UW4091. \ln/T_n is plotted as a function of depth in Figure 3 for one core from each sample. The points are fit using a luminescence exposure aging model (Sohbati et al. 2013) as explained in the caption.

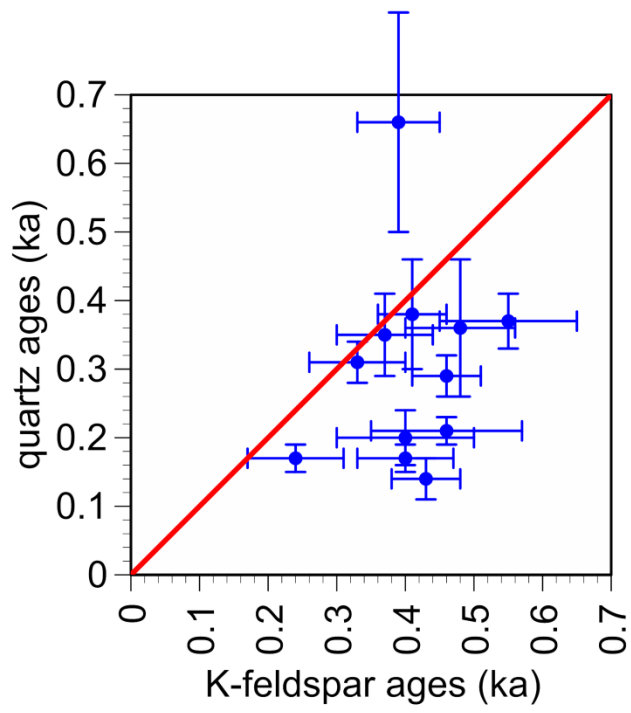
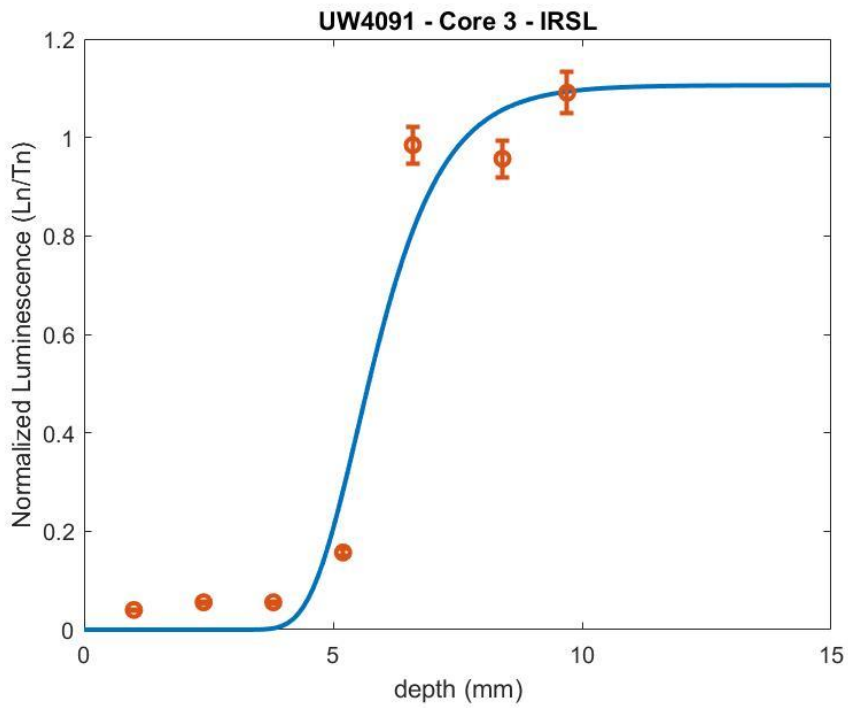


Figure 2. Comparison of K-feldspar and quartz ages. Red line is 1:1 correspondence.



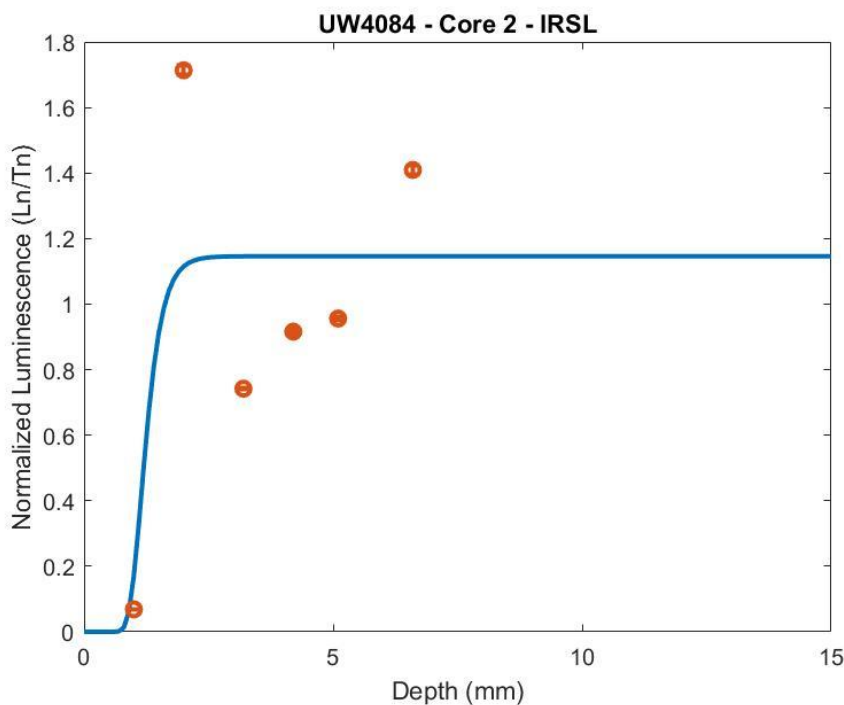


Figure 3. Depth profiles for rocks from (top) Ed Wood Cairn, RI, (UW4091) and (bottom) Hunt's Brook Souterrain, CT (UW4084). Blue lines are fits using exposure equation: $L=L_0 \exp(-\phi \sigma \circ t) \exp(-\mu x)$ where L_0 = saturation level, $\phi \sigma$ = cross-section, t = time, μ = attenuation coefficient, x =depth. Data is first formatted by measuring the weighted Ln/Tn values for each core slice, then the values are normalized to the weighted average Ln/Tn values of the deepest two slices. These data are then fitted to the model using a standard trust-region nonlinear least squares approach, utilizing arbitrary parameter values for the luminescence decay rate constant, time, and the light attenuation coefficient.

UW4091 exemplifies a rock that was well bleached at the time it was deposited in the cairn. The Ln/Tn does not change over the first 5 mm depth, indicating that sun exposure was sufficient to empty trapped charge to that depth. Beyond about 7 mm depth, the luminescence signal has not been reduced at all. UW4084, on the other hand, only shows a reduced Ln/Tn for the first slice at about 1 mm. While this may represent well-bleaching at the surface, a lack of any plateau does not guarantee it. The one quartz profile, for UW4091, shows a pattern similar to that for feldspar UW4084.

The K-feldspar age had to be corrected for anomalous fading. The fading rate did not change much with depth for either rock, averaging about 8.7 ± 0.8 %/decade for UW4091 and 6.7 ± 0.4 for UW4084. Averaging the corrected age from six slices on two cores that were within the well-bleached plateau of the depth curves produced a value FOR uw4091 of 0.54 ± 0.08 ka, or AD 1490 ± 80 , which is a little older and barely within error terms of the average K-feldspar age from the sediments. The corrected age from the surface slice of one of the cores for UW4084 is 1.03 ± 0.29 ka, or AD 990 ± 290 . This is quite a bit older than the sediment age from Hunt's Brook Souterrain (UW4083). The sample must have been only partially bleached.

The surface slice from the one core from UW4091 that had measurable OSL signals produced an age of 0.39 ± 0.04 ka, or AD 1630 ± 40 , in the range of the K-feldspar sediment ages.

4. Discussion

The rock samples provided little chronological resolution of the rock structures because most of them were poorly bleached, suggesting there was little exposure to sunlight at the time of their placement. The one rock sample that did appear well-bleached at placement yielded an age that agreed with the K-feldspar ages of the sediments. The feldspar provided a similar age for sites across New England. The quartz ages were younger and more varied. Better understanding of this discrepancy is warranted because resolution is required to show whether the structures are pre-colonial.

Quartz is known to bleach faster than feldspar, so one explanation is that the feldspar signals in these samples are less well bleached than the quartz. But the ages were based on the minimum age model, where the best bleached grains are isolated, and arguments were given earlier of why the youngest feldspar grains appeared well bleached.

Heterogeneity in the distribution of beta irradiation is a problem for single-grain dating because of the relatively short range of beta radiation compared to gamma radiation. (The effect of alpha radiation is not very significant for coarse-grain samples.) A principle cause of heterogeneity for K-feldspars is probably variation in the percentage of internal K of the feldspars themselves, which can be accounted for by increasing the error on the estimation of percent internal K. K feldspars are a principle source of beta radiation. The distribution of these is therefore a main cause of beta heterogeneity for quartz (Mayya et al. 2006). Beta radiation from the U and Th series is assumed to be more evenly distributed. Mayya et al. (2006) proposed a model, recently updated by Chauhan et al. (2021), to evaluate the effect on dose rate to individual grains in the presence of unevenly distributed K-feldspars. Others (David et al. 2007, Feathers et al. 2020) have used this model, using the proportion of beta dose rate to total dose rate and the proportion of beta dose rate stemming from K, to test whether the observed distribution of D_e values could be explained by beta heterogeneity. We applied this to seven samples using the finite mixture model (Galbraith and Roberts 2012). Using the Mayya et al. model to adjust the dose rate of the lowest component (similar to the minimum age) on the assumption these grains were far from K-feldspar hotspots, we compared the adjusted age to the age of the 2nd component (which is about the same magnitude as the central age). In no cases could the adjusted age come anywhere near to matching the age of the 2nd component, indicating that by this model beta heterogeneity could not explain the differences in D_e of the components. Nevertheless, in case this model underestimates possible heterogeneity, we increased the over-dispersion value typical of a single-age sample in the minimum age model to 25% to gauge the effect on the quartz ages. It did not make a significant difference for any sample. The biggest change, for UW4102, made a difference of only 30 years in the age. Microdosimetry does not seem able to explain the young ages of the quartz.

The quartz signal is composed of several components based on their bleachability (Jain et al. 2000). The SAR method for determining D_e in quartz was designed to work on the fast bleaching component

and is strictly applicable only to quartz signals dominated by that component (Wintle and Murray 2006). A commonly referenced model of that kind of signal is the Risø calibration quartz from a Danish beach sand. The shape of the quartz decay curves for two samples, UW4087 and UW4101, were compared with the Risø standard using linear modulated OSL (LM-OSL). In conventional OSL, the power of the stimulating laser is kept constant during measurement, but in LM-OSL the power is ramped from zero to maximum during measurement. This facilitates visual separation of the components, because the fast component empties much earlier than slower components. Here the laser was ramped from 0 to 90% power in 30s. In this mode, the Risø standard shows a sharp peak centered at about 5.4% power, dropping to a low value by 16.2% power. Where a slower bleaching component is significant, the drop from the peak value is much less. The ratio of the 16.2% signal to the 5.4% signal in the Risø standard is on average 0.29 ± 0.13 , where it is 0.55 ± 0.43 for UW4087 and 0.39 ± 0.33 for UW4101. Both samples have signals with significant slower components, although there is lots of variation. Figure 4 shows LM-OSL quartz for the three samples, selecting grains with the average ratio. UW4087 clearly has a different shape than the Risø curve. The curve for UW4101 is similar to that for Risø but has a shoulder on the main peak that probably represents a slower component. This could explain younger quartz grains in the New England samples if the young grains correlate with high ratios. However, this is not the case for UW4087 although it is the case for UW4101. For the latter sample, grains with ratios less than 0.4 (more dominance by fast component) have an average D_e of 3.4 ± 0.6 Gy compared to those with ratios greater 0.4 of 2.7 ± 0.4 Gy. Recent work (Rajapara et al. 2022) has suggested that samples with a significant slower component can underestimate the age because of sensitivity change of the natural signal.

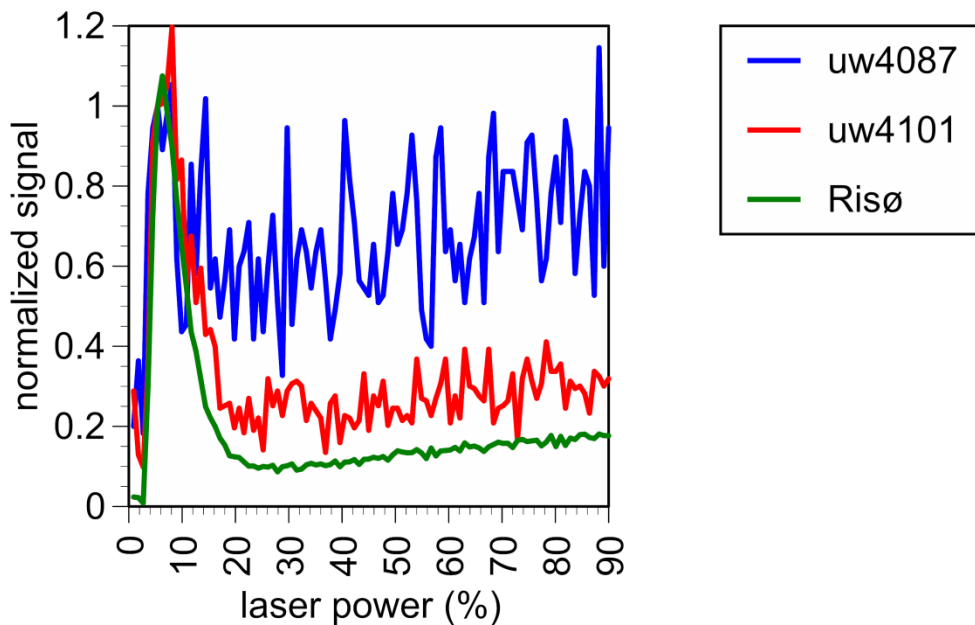


Figure 4. Normalized linear modulated OSL for three quartz grains, from UW4087, UW4101 and Risø standard. The ratios of 16.2 to 5.4% power is 0.62, 0.40, and 0.20 respectively.

Normalization is the signal at 5,4% power. Greater fluctuations in the curves for UW4087 and UW4101 are due to a much lower intensity signal compared to that for Risø.

Another way to look at this is by using the fast ratio, a ratio of signal measured early on a conventional OSL decay curve and of a signal measured later on (Duller 2012). This was done on two samples, UW4081 and UW4087, plus the Risø standard, using the signals at 0.02 s and 0.22-0.26 s, with the signal at 0.70-1.0 s subtracted as background. The ratio will increase for samples dominated by a fast component. Figure 5 shows the distribution of fast-ratio values. While mean values do not vary much, the distribution from UW4081 and UW4087 extends to much lower values than it does for the Risø standard. Also, in both UW4081 and UW4087 the ratio tended to increase with D_e , shown for UW4081 (Figure 6), although with a lot of scatter.

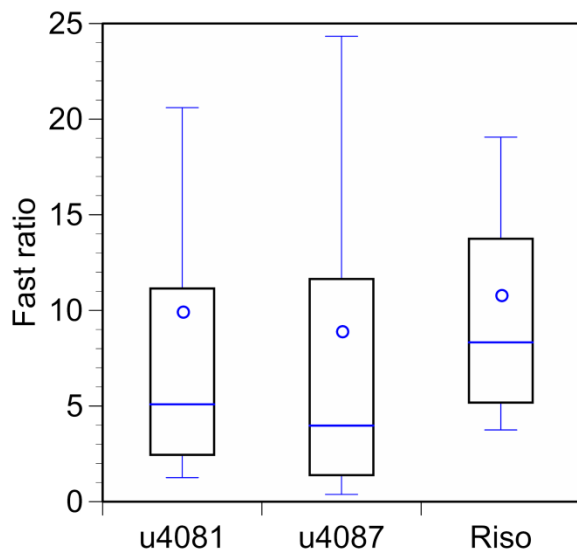


Figure 5. Box plots showing distribution of two samples plus the Risø standard. The box lines from bottom to top represent the 10th 25th, 50th (median), 75th and 90th percentiles, while the open circle represents the mean. Negative values, caused by high backgrounds are excluded. No negative values were obtained for the Risø standards, but 12 percent of UW4081 values and 24% of UW4087 values were.

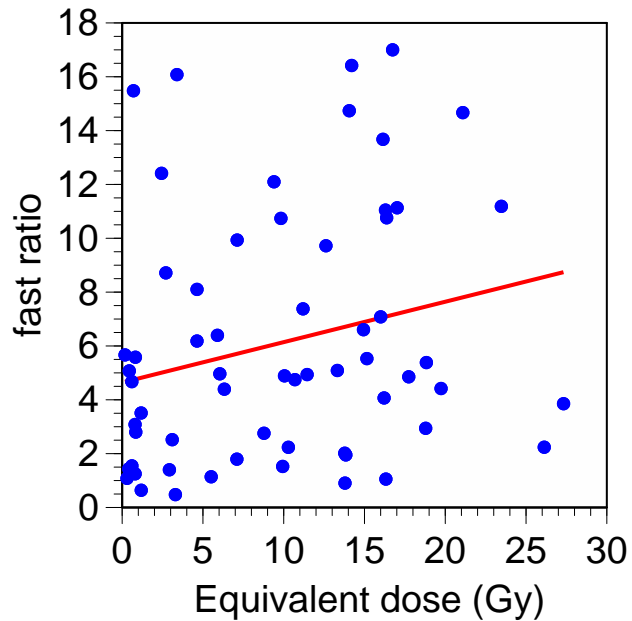


Figure 6. Fast ratio as a function of D_e (Gy) for UW4081. Fast ratios greater than 20 were excluded for ease of presentation.

The data suggest that quartz signal decay curves for many grains in the New England samples do not conform to that expected if dominated by the fast component. These data are not as conclusive as they could be because the intensities of the quartz signals are so low. Figure 7 compares the quartz and feldspar intensities for UW4081 and UW4092. The feldspar signal is 2-3 orders of magnitude larger than the quartz signals. Such low quartz signals make truly young grains difficult to distinguish from those where intensity is just too low for good resolution.

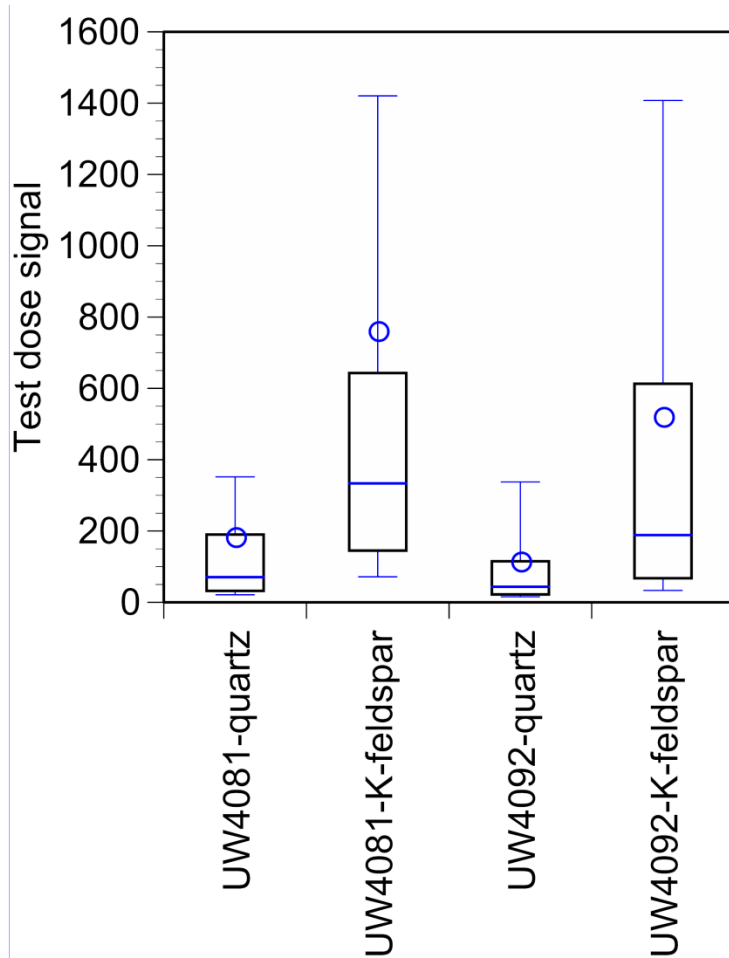


Figure 7. Box plots showing intensity of quartz versus feldspar for UW4081 and UW4092. The signal from the first test dose (about 3 Gy) was used to compare intensities. The box lines from bottom to top represent the 10th 25th, 50th (median), 75th and 90th percentiles, while the open circle represents the mean.

If the discrepancy between the quartz and feldspar signals cannot be fully explained, the quartz signals certainly have issues. The feldspar signals have fewer problems and also provide a consistency in ages that the quartz signals cannot provide. Dates on sediments obtained by Mahan (2015,2020) for Upton Chamber and Pratt Hill in Upton, MA, Tolba site near Leverett, MA, and Hopkinton Preserve, RI, range from AD 1450 to 1650, based on minimum age models. These are in the same range as the feldspar dates of $AD1590 \pm 20$ reported here. Interestingly, Mahan used mainly quartz, although some feldspar ages agreed with the quartz. There have been seven radiocarbon dates obtained at American Stonehenge and three at Gungywamp, all on charcoal, but only one of the radiocarbon dates from American Stonehenge agrees with the luminescence dates reported here.

While dating these structures does not say who built them, the dates do constrain the possibilities. The AD 1590 ± 20 date rules out colonial settlers. They began settling the coastal regions of Massachusetts in 1620-1630, but reached inland only a few decades later. There were other European visitors to the Northeast prior to AD 1620, including the Vikings (an archaeological site in Newfoundland dates to AD1000), Basque fishermen, and various English and Dutch explorers in the late 1500s and early 1600s. The French founded Quebec in 1608, following a short lived colony on Saint Croix Island in eastern Maine in 1604. But there is no evidence of sustained European settlement in New England prior to 1620. That leaves the ancestors of modern native Americans as the likely builders of the structures.

5. Conclusions

Luminescence dating was applied to sediments and rocks from several rock structures in New England. The sediments were collected from directly underneath rocks in an attempt to date the placement of the rock. The rocks were part of the structures themselves.

The radiation environment for these samples was complex, but combination of *in situ* dosimeters and laboratory measurements produced relatively consistent results for most samples.

Luminescence of the sediments was measured on single grains, using both quartz and K-feldspars. D_e was determined by SAR and the age was derived from the minimum age model. Ages were corrected for fading on the feldspars. The feldspar ages from 12 samples were consistent with a single age. The weighted average was AD 1590 ± 20. The quartz ages were systematically younger and covered a wider range of dates including some in the 19th century which did not seem credible. The quartz signals were generally weak and many of them did not appear to be dominated by the fast component. These issues cast doubt on the validity of the quartz ages. The feldspars, on the other, did not appear to have serious problems.

Of the five rocks measured, four did not appear to have been well bleached at the time of their placement. Only one rock appeared to have been well bleached and this produced an age in agreement with the feldspar ages.

The ages support building of the structures prior to colonial settlement, probably by native American groups.

Acknowledgments

This project was funded by the New England Antiquities Research Association (NEARA). Collection of the samples was organized by NEARA members, particularly through the efforts of its president, Harvey Buford. The content of the paper, however, is solely the responsibility of the authors. The analytical work was done at the University of Washington.

References

- Aitken, M. J., 1985. Thermoluminescence Dating. Academic Press, Oxford.
- Auclair, M., Lamothe, M., and Huot, S., 2003. Measurement of anomalous fading for feldspar IRSL using SAR. *Radiation Measurements* 37, 487-492.
- Banerjee, D., Murray, A. S., Bøtter-Jensen, L., and Lang, A., 2001, Equivalent dose estimation using a single aliquot of polymineral fine grains. *Radiation Measurements* 33:73-93.
- Buylaert, J-P., Jain, M., Murray, A. S., Thomsen, K. J., Thiel, C., and Sohbati, R., 2012. A robust feldspar luminescence dating method for Middle and Late Pleistocene sediments. *Boreas* 41, 435-451.
- Chauhan, N., Selvam, T. P., Anand, S., Shinde, D. P., Mayya, Y. S., Feathers, J. K., and Singhvi, A. K., 2021. Distribution of natural beta dose to individual grains in sediments. *Proceedings of the Indian National Science Academy* <https://doi.org/10.1007/s43538-021-00057-y>
- David, B., Roberts, R.G., Magee, J., Mialanes, J., Turney, C., Bird, M., White, C., Fifield, L.K., Tibby, J., 2007. Sediment mixing at Nonda Rock: investigations of stratigraphic integrity at an early archaeological site in northern Australia and implications for the human colonisation of the continent. *J. Quat. Sci.* 22, 449–479.
- Duller, G. A. T., 2012. Improving the accuracy and precision of equivalent doses determined using the optically stimulated luminescence signal from single grains of quartz. *Radiation Measurements* 47, 770-777.
- Feathers, J. K., Zedeño, M. N., Todd, L., and Aaberg, S. A., 2015, Dating stone alignments by luminescence. *Advances in Archaeological Practice* 3: 378-396.
- Feathers, J. K., More, G., Solis, P., and Burkholder, J. E., 2019. IRSL dating of rocks and sediments from desert geoglyphs in coastal Peru. *Quaternary Geochronology* 49:177-183.
- Feathers, J. K., Evans, M., Stratford, D. J., and de la Peña, P., 2020. Exploring complexity in luminescence dating of quartz and feldspars at the Middle Stone Age site of Mwulu's Cave (Limpopo, South Africa). *Quaternary Geochronology* <https://doi.org/10.1016/j.quageo.2020.101092>
- Galbraith, R. F., and Roberts, R. G., 2012. Statistical aspects of equivalent dose and error calculation and display in OSL dating: an overview and some recommendations. *Quaternary Geochronology* 11:1-27.
- Hoffman, C., 2019. Stone prayers: native American constructions of the eastern seaboard. Arcadia Publishing, West Columbia, SC.
- Ives, T. H., 2013. Remembering stone piles in New England. *Northeast Anthropology* 79-80, 37-80.
- Ives, T. H., 2015. Cairnfields in New England's forgotten past. *Archaeology of Eastern North America* 43, 119-132.

- Jain, M., Murray, A. S., and Bøtter-Jensen, L., 2003. Characterization of blue-light stimulated luminescence components in different quartz grains: implications for dose measurement. *Radiation Measurement* 37, 441-449.
- Huntley, D. J., and Lamothe, M., 2001. Ubiquity of anomalous fading in K-feldspars and the measurement and correction for it in optical dating. *Canadian Journal of Earth Sciences* 38, 1093-1106.
- Mahan, S. A., 2020. Optically stimulated luminescence (OSL) data and ages for selected native American stone landscape features: final project report submitted to the Narragansett Indian Tribal Historic Preservation Trust. U. S. Geological Survey, Department of the Interior, USA
- Mahan, S. A., Martin, F., and Taylor, C., 2015. Construction ages of the Upton Stone Chamber: preliminary findings and suggestions for future luminescence research. *Quaternary Geochronology* 30, 422-430
- Mayya, Y., Morthekai, P., Murari, M.K., Singhvi, A., 2006. Towards quantifying beta microdosimetric effects in single-grain quartz dose distribution. *Radiat. Meas.* 41, 1032–1039.
- Moore, C. M., and Weiss, M. V., 2016. The continuing “stone mound problem”: identifying and interpreting the ambiguous rock piles of the Upper Ohio Valley. *Journal of Ohio Archaeology* 4,39-71.
- Murray, A. S., and Wintle, A. G., 2000, Luminescence dating of quartz using an improved single-aliquot regenerative-dose protocol. *Radiation Measurements* 32, 57-73.
- Singhvi, A. K., Rajapara, H. M., Chauhan, N., Feathers, J., Garnett, S., Wasson, R. J., Jairwal, M. K., and Gajjar, P. N., 2022. How robust are SAR single grain paleo-doses: the role of sensitivity changes? *Quaternary Geochronology* submitted
- Smedley, R.K., Duller, G.A.T., Pearce, J.G., Roberts, H.M., 2012. Determining the K-content of single-grains of feldspar for luminescence dating. *Radiat. Meas.* 47, 790–796.
- Sohbati, R., Murray, A. S., Chapot, M. S., Jain, M., & Pederson, J. (2012). Optically stimulated luminescence (OSL) as a chronometer for surface exposure dating. *Journal of Geophysical Research: Solid Earth*, 117(B9).
- Wintle, A. G., and Murray, A. G., 2006, A review of quartz optically stimulated luminescence characteristics and their relevance to single-aliquot regeneration dating protocols. *Radiation Measurements*, 41, 3639-391